Journal of Alloys and Compounds 509 (2011) L129–L133

Contents lists available at ScienceDirect

Journal of Alloys and Compounds

journal homepage: www.elsevier.com/locate/jallcom

Letter

Preparation of $Cu(In,Ga)Se_2$ thin films by pulse electrodeposition

Fangyang Liu*, Chun Huang, Yanqing Lai*, Zhian Zhang, Jie Li, Yexiang Liu

School of Metallurgical Science and Engineering, Central South University, Changsha 410083, China

ARTICLE INFO

Article history:
Received 19 June 2010
Available online 13 December 2010

Keywords:
Cu(In
Ga)Se_2
Thin films
Pulse electrodeposition
Duty cycle
Nucleation and growth

ABSTRACT

$Cu(In,Ga)Se_2$ thin films were prepared from aqueous solution by pulse electrodeposition. It was found that the co-deposition of the species occurred under a 3D growth with instantaneous nucleation. The morphology of the pulse-electrodeposited film can be improved by adjusting the duty cycle. The significant loss of indium and reduction of In–Se compound(s) accordingly were observed with decrease of duty cycle. Chalcopyrite structure $Cu(In,Ga)Se_2$ films with p-type behavior and enhancement in crystallinity were obtained after annealing treatment in Ar atmosphere.

1. Introduction

$Cu(In, Ga)Se_2$ (CIGS) is a very promising semiconductor material for solar cell [1,2] and photoelectrochemical hydrogen production application [3]. Thin film CIGS solar cell devices, fabricated from a multistep physical vapor deposition (PVD) process, have demonstrated a record conversion efficiency of 20.3% [4]. The PVD technology is excellent for good quality film growth, but difficult to scale up. There is thus great interest in developing low cost non-vacuum-based techniques such as electrodeposition [5]. Several studies on electrodeposition of CIGS thin film have been reported [6–8], and these studies have mainly focused on the potentiostatic electrodeposition technique using direct current (DC) mode. There are very few research that attempts to achieve pulse electrochemical growth of CIGS films [9] but fails to incorporate gallium into the films during electrodeposition, even if ternary $CuInSe_2$ thin film prepared by pulse electrodeposition have been reported [10–12]. Pulsed electrodeposition is an advanced form of electrodeposition, which offers better control over deposit properties by controlling the interfacial electrochemical reaction for the formation of CIGS. In contrast to the DC electrodeposition where only potential or current can be controlled, in pulse electrodeposition, a number of variables like pulse waveform, cathodic/anodic pulses, on/off pulse time or duty cycle θ, and applied potential, etc. [13] can be independently varied and offer effective ways to control properties such as microstructure, adhesion, composition, crystallinity, optical and electrical properties. On the other hand, the study of the mechanism of CIGS electrodeposition is very insufficient [14], especially the nucleation and growth mechanism of CIGS during deposition has not been reported to our knowledge, although an understanding of CIGS nucleation and growth mechanism will help in producing CIGS deposits with desirable properties.

In this work, $Cu(In,Ga)Se_2$ thin films were pulse electrodeposited from acidic solution. The preliminary results of investigation of the electrochemical nucleation and growth mechanism by cyclic voltammetry and chronoamperometry, as well as film composition, morphology and structure properties were presented.

2. Experimental

The electrochemical analyses, including cyclic voltammetric (CV) and chronoamperometric (CA) measurements, and electrodeposition of Cu–In–Ga–Se films were performed in a typical three-electrode cell where the working electrode was Mo/glass(Mo film thickness ≈0.7 μm and active area = 1 cm × 1 cm), the counter electrode was a platinum plate, and the reference electrode was a saturated calomel electrode (SCE). All potentials are reported with respect to this reference. The electrolyte bath contained 3 mmol/L $CuCl_2$, 10 mmol/L $InCl_3$, 10 mmol/L $GaCl_3$, 8 mmol/L H_2SeO_3 and 60 mmol/L sodium sulfamate as complexing agent, which can hinder the formation of copper selenides [15]. The pH of the solution was adjusted to 2.10–2.20 using concentrated hydrochloric acid (HCl). All electrochemical experiments were carried out in this electrolyte bath using a Princeton applied research 2273 A potentiostat at room temperature (25 °C) and without stirring. The deposition of the CIGS films was performed with a square-pulse potential where nonpulse potential E_o was constant at 0.0 V, and pulse potential was constant at −0.6 V according to the results of CV measurement. The pulse period T ($T = t_{on} + t_{off}$) was constant at 3 s and duty cycle θ $\left(\theta = \frac{t_{on}}{t_{on}+t_{off}} \times 100\%\right)$ varied from 33 to 100%. The deposition time was 60 min in all the cases. The thickness of the films, estimated by SEM, was found to vary between 0.8 and 1.5 μm according to the duty cycle. Residual oxygen in the bath was removed by N_2 bubbling for 20 min prior to the electrochemical measurements and electrodeposition. The as-deposited films were annealed in Ar

* Corresponding authors. Tel.: +86 731 8830474; fax: +86 731 8876454.
E-mail addresses: liufangyang1984@126.com (F. Liu), csulightmetals@126.com (Y. Lai).

0925-8388/$ – see front matter © 2010 Elsevier B.V. All rights reserved.
doi:10.1016/j.jallcom.2010.12.031

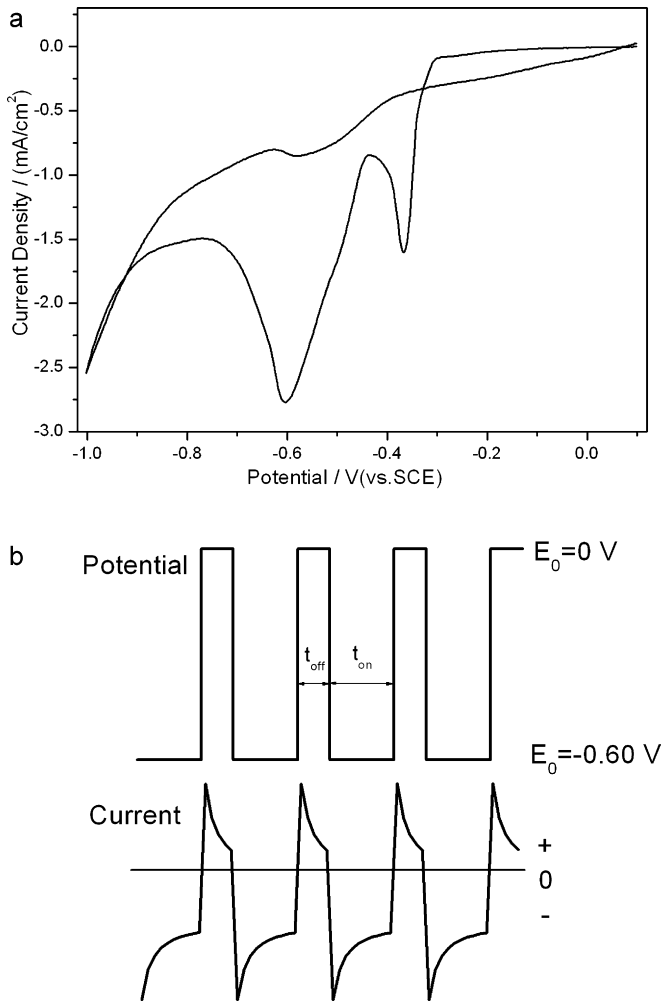

Fig. 1. (a) A typical cyclic voltammogram of an electrolyte bath containing 3 mmol/L $CuCl_2$, 10 mmol/L $InCl_3$, 10 mmol/L $GaCl_3$, 8 mmol/L H_2SeO_3 and 60 mmol/L sodium sulfamate on Mo/glass electrode at pH 2.2 and scan rate of 10 mV/s. (b) An illustration of pulse waveforms of cathode potential and the corresponding current for electrodeposition.

ambient at 500 °C for 10 min to form Cu(In,Ga)Se_2 and improve their crystalline properties.

The chemical composition, surface morphology and crystalline properties of the prepared films were characterized by energy dispersive X-ray spectroscopy (EDS, EDAX-GENSIS60S), scanning electron microscopy (SEM, JSM-6360LV) and X-ray diffraction (XRD, Rigaku3014), respectively. The photoelectrochemical characterization of the films was carried out in 0.5 M H_2SO_4 solution using a 300 W xenon arc lamp as the light source with light intensity kept at 100 mW cm^{-2}, referring the potential again to the SCE, to study their photosensitivity as well as conductivity type.

3. Results and discussion

Fig. 1(a) illustrates the typical cyclic voltammogram for co-deposition of quaternary Cu–In–Ga–Se film. As seen in Fig. 1(a), the curve displays two well-defined cathodic peaks, two anodic peaks and a double crossing between the cathodic and anodic branches. The first cathodic peak between −0.30 V and −0.43 V corresponds to the formation of Cu–Se binary compound(s) and the second cathodic peak at about −0.6 V is attributed to the co-deposition of Cu, In, Ga and Se according to the composition of films deposited at relevant potential (region) determined by EDS analysis. Similar electrochemical characteristics also have been observed by others for $CuInSe_2$ [16] and Cu(In,Ga)Se_2 [17] electrodeposition. After the second peak, a further negative shift in potential results in the decrease of the cathodic current density until the potential reaches −0.76 V, where the evolution of hydrogen begins. The anodic peaks at about −0.63 V and −0.38 V may correspond to the oxidation of hydrogen and incorporated In or Ga or their selenides, respectively. No other anodic peaks for dissolution of Cu–Se compound(s) are seen in the cyclic voltammogram probably because the potentials are not positive enough. The presence of the double crossover of the reverse anodic scan over the cathodic scan, giving rise to what has been called the "nucleation loop", is diagnostic for the nuclei formation on the electrode surface [18]. The crossover positions of this double crossover are at about −0.36 V and −0.91 V, respectively. It shows that the nucleation occurs when the potential is negative than −0.36 V, and the mode of the nucleation or the kind of the nuclei may vary after −0.91 V. Based on assignment of the reductive peaks and the occurrence of nucleation for potentials negative than −0.36 V, the pulse potential was selected to be −0.60 V and the typical potential–time curve and the corresponding current–time behavior are shown in Fig. 1(b). It can be observed easily that although these potential pulses are of square in shape, the corresponding current form is differently modulated due to the presence of an electric double layer at the cathode–electrolyte interface forming a capacitor of molecular dimension [19]. It is also found that the current changes from negative during t_{on} to positive during t_{off}, which means that the film plating process, in our experimental conditions, is a well-balanced repetition of cathodic deposition and anodic dissolution actually.

The nucleation and growth mechanisms during the codeposition of the species on the plain carbon steel have been studied using Scharifker and Hill's so-called instantaneous and progressive nucleation models [20]. The models for the instantaneous and the progressive nucleation are given by Eqs. (1) and (2), respectively.

$$\left(\frac{i}{i_m}\right)^2 = 1.9542\left(\frac{t}{t_m}\right)^{-1}\left\{1-\exp\left[-1.2564\left(\frac{t}{t_m}\right)\right]\right\}^2 \quad (1)$$

$$\left(\frac{i}{i_m}\right)^2 = 1.2254\left(\frac{t}{t_m}\right)^{-1}\left\{1-\exp\left[-2.3367\left(\frac{t}{t_m}\right)^2\right]\right\}^2 \quad (2)$$

where I_m and t_m are the current and time coordinates, respectively, at the peak maximum in the current transient. Fig. 2(a) shows the current transient for co-deposition of Cu–In–Ga–Se film. This current transient was obtained by stepping the cathodic potential from 0.2 V, where deposition does not occur, to potential of −0.60 V, where would be minimum interference from the hydrogen evolution as can be seen in Fig. 1(a). The relation of dimensionless variables (I/I_m) and (t/t_m) derived from experimental current transient and the theoretical ones are shown in Fig. 2(b). It is shown that the experimental data are in good agreement with the grow law for instantaneous nucleation followed by diffusion-limited growth before reaching the maximum points. However, for long time $(t \gg t_m)$, experimental current density falls lower (negative deviation) than would be predicted by the growth of hemispheroids. A lack of agreement between theory and experiment for $t > t_m$ in potentiostatic current transients has been reported for many systems and the disagreement was accounted for in terms of death and rebirth of crystal growth [21], overlap of diffusion zones [22] or concurrent hydrogen evolution [23]. Nevertheless, it should be note that experimental current density values are always larger than the predictions of the model (positive deviations) in those cases. Therefore, a different source of error has to be considered in our work, whereas an adequate explanation for negative deviation is not available up to now. In the present work, the passivation of the electrode resulting from the poor conductivity of deposit is reasonably considered to be the possible reason. Consequently, considering the electrode passivation, it can be believed that CIGS electrodeposition is carried out under a 3D growth with instantaneous nucleation.

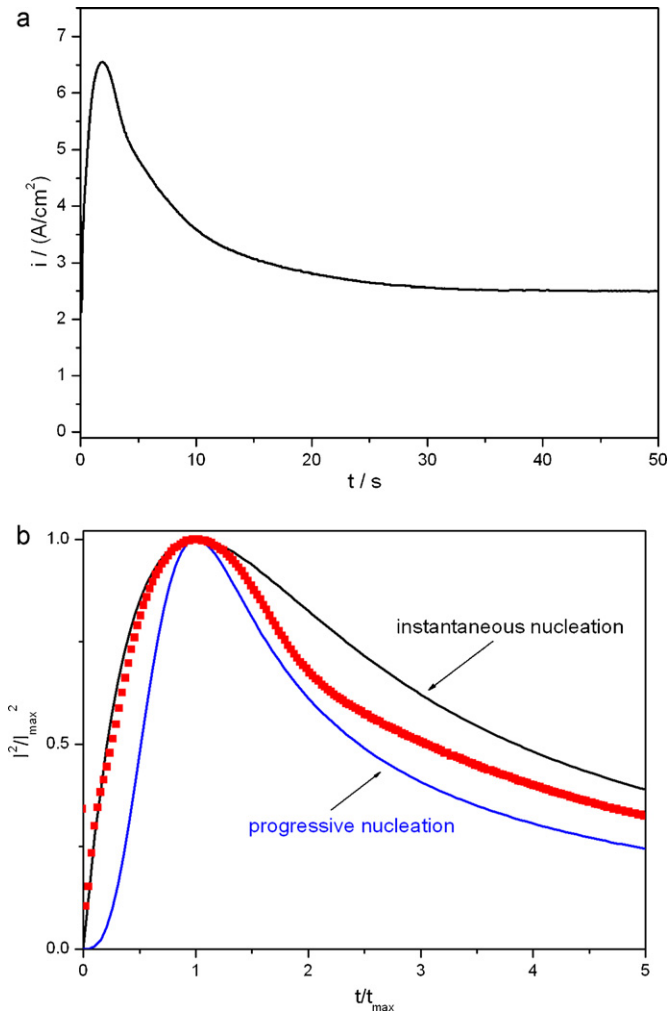

Fig. 2. (a) A typical current–time transient from an electrolyte bath containing 3 mmol/L $CuCl_2$, 10 mmol/L $InCl_3$, 10 mmol/L $GaCl_3$, 8 mmol/L H_2SeO_3 and 60 mmol/L sodium sulfamate on Mo/glass electrode at pH 2.2 and applied potential of −0.6 V. (b) Dimensionless curves $(i/i_m)^2$ vs. t/t_m for instantaneous and progressive 3D nucleation from Eqs. (1) and (2), respectively, along with experimental data.

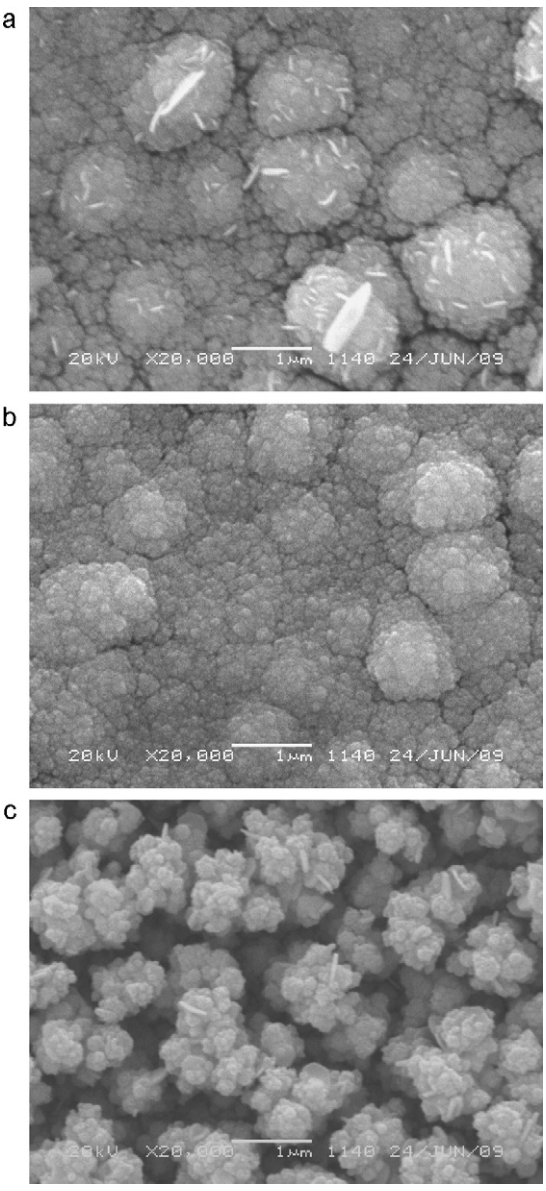

Fig. 3. Surface morphologies of pulse electrodeposited CIGS film from an electrolyte bath containing 3 mmol/L $CuCl_2$, 10 mmol/L $InCl_3$, 10 mmol/L $GaCl_3$, 8 mmol/L H_2SeO_3 and 60 mmol/L sodium sulfamate on Mo/glass electrode at pH 2.2 and various duty cycle θ: (a) $\theta = 100\%$, (b) $\theta = 67\%$, (c) $\theta = 33\%$.

The compositions of the electrodeposited films determined by EDS measurement and normalized to Cu = 1 at duty cycle θ of 100% (i.e. potentiostatic electrodeposition), 67% and 33% are $CuIn_{0.65}Ga_{0.34}Se_{2.12}$, $CuIn_{0.51}Ga_{0.36}Se_{1.96}$ and $CuIn_{0.12}Ga_{0.27}Se_{1.69}$, respectively. This result is indicative that decreasing of duty cycle from 100% to 67% reduces the relative content of In and Se, but has no obvious effect on Ga relative content in the film. Taking into account the current–time behavior during pulse electrodeposition in Fig. 1(b), this can be attributed to the fact that In was first dissolved back into the solution due to its lowest electronegativity corresponding to the positive current during the nonpulse duration t_{off}, leading to the loss of In in deposited film, and therefore reduction of In–Se compound(s). Similar phenomenon also has been reported during the pulse electrodeposition of ternary $CuInSe_2$ [24]. When duty cycle further decreases to 33%, besides significant loss of In, the relative content of Ga also indicates some drop, thereby leading to a corresponding reduction of Ga–Se compound(s).

Surface morphologies of the electrodeposited films were observed using SEM as show in Fig. 3. For duty cycle of 100%, the film shows a non-uniform morphology with dendritic structure (Fig. 3(a)), which is often produced during potentiostatic electrodeposition easily owing to concentration polarization [25]. When duty cycle decreases to 67%, the deposited film is homogeneous in appearance (Fig. 3(b)), which is attributed to the selective dissolution of the projecting parts with high electrochemical activity from the film surface. With further decreasing of duty cycle to 33%, the excessive dissolution back during a quite long t_{off} results in the depletion of the film bulk and a corresponding rather rough surface (Fig. 3(c)) which is not fit for application.

Fig. 4(a) displays a comparison of XRD patterns measured for pulse electrodeposited CIGS film with a composition of $CuIn_{0.71}Ga_{0.34}Se_{2.18}$ before and after annealing. The spectra of the as-deposited film presents only three weak broad peaks at about $2\theta = 26.7^\circ$, 44.3° and 52.5°, suggesting an extremely poor degree of crystallinity. For annealed film, an improvement in the sharpness and intensity of the diffraction peaks can be due to the recrystallization and grain growth. It can be seen that the annealed film has the basic chalcopyrite structure, which confirmed by the minor peaks labeled (1 0 1), (1 0 3), (2 1 1), and (3 1 6), etc. [26,27]. No evidence of secondary phases was observed from the XRD data. Furthermore, it is very important to remark that the (1 1 2) peak at $2\theta = 26.9^\circ$ is

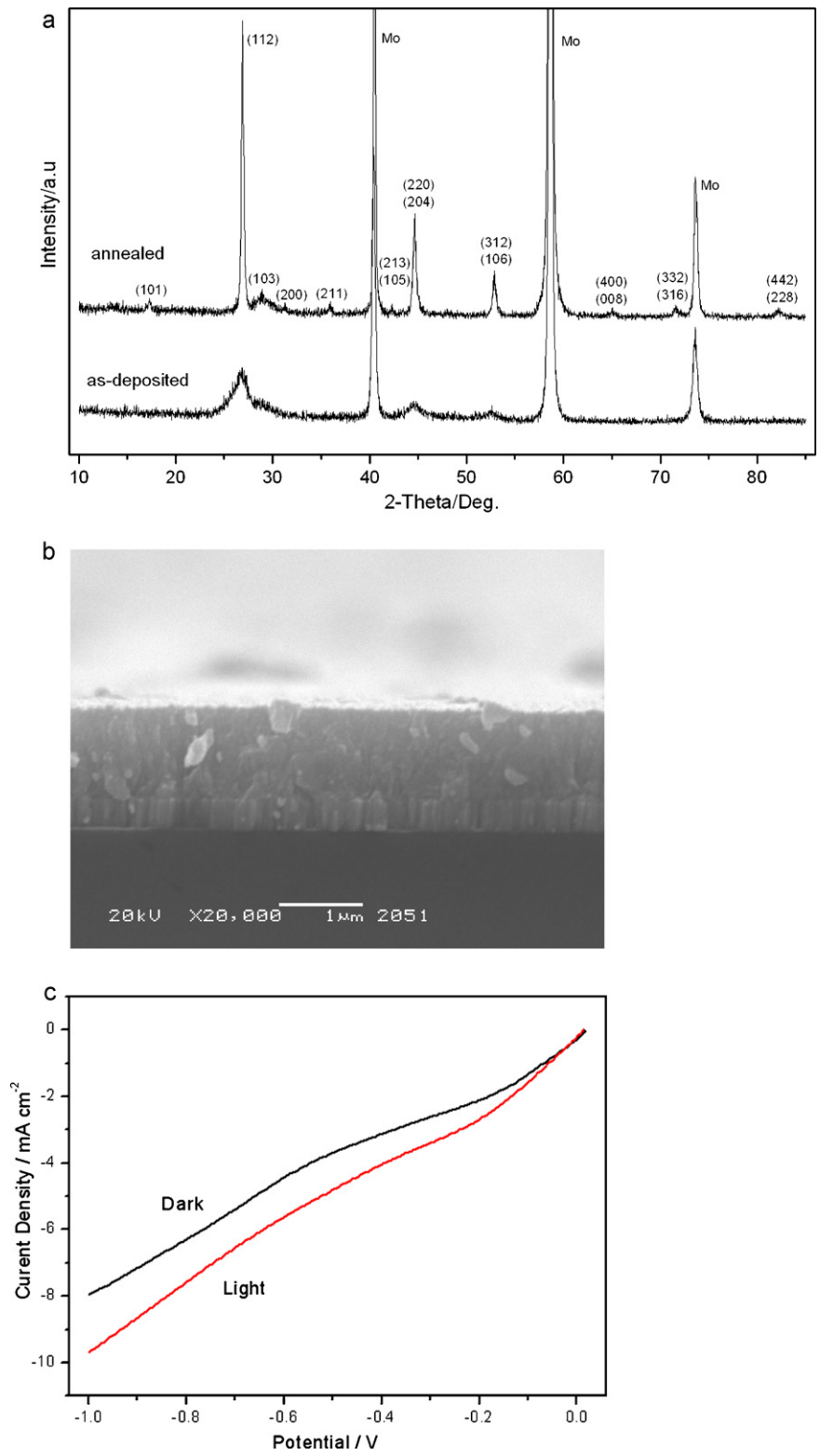

Fig. 4. (a) A comparison of XRD patterns measured for typical pulse electrodeposited CIGS film from an electrolyte bath containing 3 mmol/L $CuCl_2$, 10 mmol/L $InCl_3$, 10 mmol/L $GaCl_3$, 8 mmol/L H_2SeO_3 and 60 mmol/L sodium sulfamate on Mo/glass electrode at pH 2.1 and duty cycle of 67% before and after annealing. (b) The SEM image of cross section of the annealed CIGS film. (c) The photocurrent versus electrode potential for the annealed CIGS film in a photoelectrochemical cell configuration. Scan rate = 10 mV/s.

higher than that of $CuInSe_2$ ($2\theta = 26.6^\circ$), which is owing to the fact that the formation of quaternary CIGS with substitution of In by Ga brings a decrease in the lattice parameters and therefore d-spacings of the material. This substitution of In by Ga can also widen the band gap from 1.01 eV for $CuInSe_2$ to 1.17 eV for this $CuIn_{0.71}Ga_{0.34}Se_{2.18}$ sample based on the composition to band gap relation [28,29]. In order to get insight into its microstructure profile, the cross section of the annealed CIGS film is present, as shown in Fig. 4(b). It can be seen that the film with a thickness of about 1 μm and a very compact and homogeneous morphology having large grains

extending from the back to the front of the film has been grown on the substrate.

The annealed film was further analyzed by photoelectrochemical (PEC) test, as shown in Fig. 4(c). It is exhibited that the cathode photocurrent is increased in the direction of the cathode potential, which is a characteristic of a semiconductor with p-type conductivity. It is also seen that the photocurrent increases very slowly without arriving at a saturated value, which are very similar to those reported in earlier published results [30]. This behavior is attributed to the recombination of charge carries at the grain boundary of the semiconductor, which results in low photoconversion efficiency.

4. Conclusions

Cu(In,Ga)Se_2 thin films were pulse-electrodeposited from aqueous solution. The cyclic voltammetric studies show the potential range for Cu, In, Ga and Se co-electrodeposition and the chronoamperometric investigation reveals the instantaneous nucleation and 3D diffusion controlled growth mode for co-electrodeposition. The pulse-electrodeposited films show the best morphology for duty cycle of 67%. With the decrease of duty cycle, significant loss of indium, and reduction of In–Se compound(s) accordingly can be observed. Chalcopyrite structure Cu(In,Ga)Se_2 film with a band gap of about 1.17 eV and p-type behavior and enhancement in crystallinity were obtained after annealing treatment in Ar atmosphere.

References

[1] P.P. Hankare, K.C. Rathod, P.A. Chate, A.V. Jadhav, I.S. Mulla, J. Alloys Compd. 500 (2010) 78.
[2] E. Lee, J.W. Cho, J. Kim, J. Yun, J.H. Kim, B.K. Min, J. Alloys Compd. 506 (2010) 969.
[3] L. Djellal, S. Omeiri, A. Bouguelia, M. Trari, J. Alloys Compd. 476 (2009) 584.
[4] http://www.pv-tech.org/news/_a/zsw_sets_another_new_cigs_997_solar_cell_record/.
[5] P. Cojocaru, L. Magagnin, E. Gómez, E. Vallés, J. Alloys Compd. 503 (2010) 454.
[6] L. Zhang, F.D. Jiang, J.Y. Feng, Sol. Energy Mater. Sol. Cells 80 (2003) 483.
[7] N.B. Chaure, A.P. Samantilleke, R.P. Burton, J. Young, I.M. Dharmadasa, Thin Solid Films 472 (2005) 212.
[8] M.E. Calixto, K.D. Dobson, B.E. McCandless, R.W. Birkmire, J. Electrochem. Soc. 153 (2006) G521.
[9] R.N. Bhattacharya, W. Batchelor, J.E. Granata, F. Hasoon, H. Wiesner, K. Ramanathan, J. Keane, R.N. Noufi, Sol. Energy Mater. Sol. Cells 55 (1998) 83.
[10] F. Kang, J. Ao, G. Sun, Q. He, Y. Sun, J. Alloys Compd. 478 (2009) L25.
[11] C.D. Lokhande, J. Electrochem. Soc. 134 (1987) 1727.
[12] J. Yang, Z. Jin, C. Li, W. Wang, Y. Chai, Electrochem. Commun. 11 (2009) 711.
[13] R.K. Sharma, G. Singh, A.C. Rastogi, Sol. Energy Mater. Sol. Cells 82 (2004) 201.
[14] Y.Q. Lai, F.Y. Liu, Z.A. Zhang, J. Liu, Y. Li, S.S. Kuang, J. Li, Y.X. Liu, Electrochim. Acta 54 (2009) 3004.
[15] J. Liu, F. Liu, Y. Lai, Z. Zhang, J. Li, Y. Liu, J. Electroanal. Chem. (2010), doi:10.1016/j.jelechem.2010.10.021.
[16] F. Chraibi, M. Fahoume, A. Ennaoui, J.L. Delplancke, Phys. Status Solidi (a) 186 (2001) 373.
[17] M.E. Calixto, K.D. Dobson, B.E. McCandless, R.W. Birkmire, Mater. Res. Soc. Symp. Proc. 865 (2005) F14.17.1.
[18] R. Greef, R. Peat, L.M. Peter, D. Pletcher, J. Robinson, Instrumental Methods in Electrochemistry, Ellis Horwood, Chichester, 1985, pp. 283.
[19] W.H. Berttain, P.J. Boody, J. Electrochem. Soc. 107 (1962) 574.
[20] B. Scharifker, G. Hills, Electrochim. Acta 28 (1983) 879.
[21] M.Y. Abyaneh, M. Fleischmann, J. Electroanal. Chem. 119 (1981) 187.
[22] M.Y. Abyaneh, J. Electroanal. Chem. 586 (2006) 196.
[23] M. Palomar-Pardaé, B.R. Scharifker, E.M. Arce, M. Romero-Romo, Electrochim. Acta 50 (2005) 4736.
[24] S. Endo, Y. Nagahori, S. Nomura, Jpn. J. Appl. Phys. 85 (1996) L1101.
[25] M. Paunovic, M. Schlesinger, Fundamentals of Electrochemical Deposition, Wiley-Interscience, New Jersey, 1998, pp. 167.
[26] F.J. Pern, R. Noufi, A. Mason, A. Franz, Thin Solid Films 202 (1991) 299.
[27] H. Gomez, R. Schrebler, L. Basaez, E.A. Dalchiele, J. Phys. Condens. Matter 5 (1993) A349.
[28] M. Alonso, M. Garriga, C. Durante Rincón, E. Hernández, M. León, Appl. Phys. A 74 (2002) 659.
[29] A.V. Mudryi, I.A. Victorov, V.F. Gremenok, A.I. Patuk, I.A. Shakin, M.V. Yakushev, Thin Solid Films 431–432 (2003) 197.
[30] A.M. Fernandez, P.J. Sebastian, M.E. Calixto, S.A. Gamboa, O. Solorza, Thin Solid Films 298 (1997) 92.